Invited Paper

Photonics and Flexible Display Applications of Phase-Separated Liquid Crystals

Kwang-Soo Bae[a], Yoonseuk Choi[b] , Min Young Jin[d], Jong-Wook Jung[e], and Jae-Hoon Kim[*a,b,c]
[a]Department of Information Display Engineering, Hanyang University,
[b]Research Institute of Information Display, Hanyang University,
[c]Department of Electronics and Computer Engineering, Hanyang University,
17 Haengdang-Dong, Seongdong-Gu, Seoul 133-791, Korea;
[d]Image Lab Corp., Sa-dong, Ansan-si, Gyenggi-do, 426-791, Korea ;
[e]LG-Philips LCD, 163-1, Simi-dong, Gumi-si, Gyungsangbuk-do, 730-731, Korea

ABSTRACT

Anisotropic phase-separation of liquid crystal and polymer composite is highly applicable for obtaining the durable electro-optic devices. In this presentation, the theoretical model for phase separation phenomena based on the one-dimensional kinetic approach is introduced. For the applications of phase-separated LCs, we propose the fabrication of mechanically stable flexible display and electrically controllable microlens array using two- or three-dimensional anisotropic phase separation. Since LC molecules are isolated by polymer structure due to the anisotropic phase separations, resultant devices show very good mechanical stability against external pressure and stable electro-optic characteristics.

Keywords: phase separation, flexible display, microlens array, liquid crystal, polymer

1. INTRODUCTION

Recently, new methods to prepare liquid crystal (LC)-based electro-optic (EO) devices by anisotropic phase separation of LC gather great interests. In the phase separation, the LC is mixed with low molecular-weight monomers or oligomers which act as a solvent for the LC. By the application of heat, radiation, or light, the monomers can be polymerized and the LC is expelled from the polymerized volume. In particular, the photo-initiated polymerization is very powerful and widely used for fabricating various EO devices due to the ease control of polymerization and the simple patterning capability. Since the method can control the phase separation process using spatial distribution of ultra violet (UV) intensity and surface wetting properties, it is possible to develop various shapes of microstructures.

Depending on the various parameters including the concentration, temperature of the phase separation, the spatial gradient in the rate of polymerization and the diffusion coefficients of the materials, several different structures can be produced as shown in Fig. 1. At low polymer concentrations, a polymer stabilized cholesteric texture (PSCT) or cellular structures are obtained [7]. At higher polymer concentrations, the resultant structures depend on the rate and the nature of the phase separation. At a fast rate, the phase separation occurs in the whole area of the sample and the LC droplets are formed and dispersed in the polymer structure. It is named as a polymer-dispersed LC (PDLC) [7]. This structure is quite durable and stable but requires a high operation voltage for EO devices.

The simplest case of the method is fabrication of phase-separated composite organic film (PSCOF) [1] which has multilayer structures of LC and polymer. When the polymerization occurs slowly, the LC droplets become larger and are finally dispelled from the surrounding polymers due to an anisotropic phase separation. Using PSCOFs, we can obtain various shapes of polymer structures, for example, polymer walls and relief structures which is easy to fabricate and durable for mechanical stress. Moreover, if we can produce and control UV intensity modulation in two-dimension, we can make multi-dimensional structure very easily by the anisotropic phase separation.

Emerging Liquid Crystal Technologies III, edited by Liang-Chy Chien,
Proc. of SPIE Vol. 6911, 69110H, (2008) · 0277-786X/08/$18 · doi: 10.1117/12.762436

In this paper, we will introduce the applications of an anisotropic phase separation in a LC/polymer composite. A mechanically stable flexible LC display with polymer structures, fabricated using the anisotropic phase separation, is demonstrated. As an example of two- or three-dimensional anisotropic phase separation, a dynamic LC microlens array will be reported.

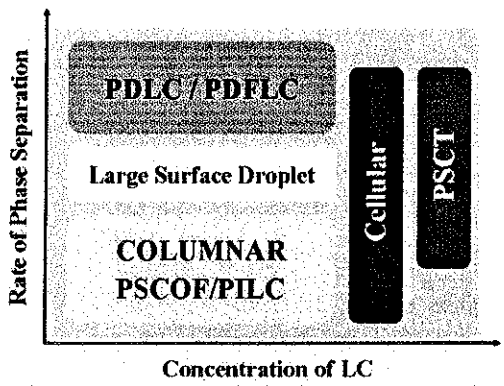

Fig. 1. Diagram of the phase separation depending on the concentration and the rate of the phase separation.

2. PHASE SEPARATED COMPOSITE FILM

An anisotropic phase separation method using the PIPS is useful for fabricating the PSCOF of the LC and a polymer [1]. This PSCOF structure, in general, has adjacent uniform layers of the LC and the polymer parallel to substrates. As we have mentioned in the previous section, the construction of PSCOF structure are highly depend on the various parameters. The rate of phase separation, which can be controlled by varying the intensity, and surface wetting properties, are the most important factor in determining the resultant structure. Two samples, with 40 wt% of the LC Felix-15-100 commercial mixture (Hoechst, Germany) and 60 wt% prepolymer NOA-65 (Norland, USA), were prepared to observe the effect of UV exposure on the final structure. The mixtures were introduced into a sandwiched cell by capillary action at a temperature well above the clearing point of the LC. Two glass substrates with transparent electrodes were sandwiched by using the spacers. Cell gap was 5 μm. All components of the LC mixtures we used are miscible with the prepolymer and immiscible with the polymer. The phase separation was initiated by exposing the cell to the UV light through the substrate having no alignment layer. The UV light was illuminated at the intensity of 200 W for about 5 min.

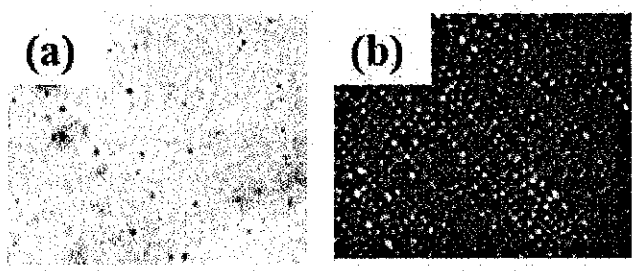

Fig. 1. Photographs taken through a microscope with samples between crossed polarizers. The UV dosage of (a) and (b) are 0.75 and 20 mJ/cm^2, respectively.

Microscopic textures shown in Figs. 2(a) and (b) illustrate how the resultant structure changes from PSCOF to PDLC as the total UV dosage applied in a given time varies over the range 0.75 and 20 mJ/cm^2, respectively. It is seen that high irradiance leads to the formation of heterogeneous structures characteristic of a PDLC. The diameters of the droplets visible in Fig. 2(b) are of the order of 2–4 μm. The PSCOF structure formed at low irradiance gives a nearly uniform optical texture Fig. 2(a).

In order to explain the mechanism responsible for the anisotropic phase separation of LCs by photo-reaction, we had developed a one-dimensional theoretical model that is based on the kinetic approach [8]. In this model, the formation of PSCOF structure can be understood by the non-uniform polymerization [9] (i.e., the diffusions of monomers and LCs and the gradient polymerization process in the mixtures). In this model, the phase separation depends on the concentrations of three constituents in the mixture; the volume fractions of the LC, the prepolymer, and the immobile polymer. Since we consider the UV irradiation is very uniformly performed, these three parameters are assumed to be functions time, and of distance, from the bottom substrate. The total volume is assumed to be constant and initially the three compounds are uniformly dispersed in the medium.

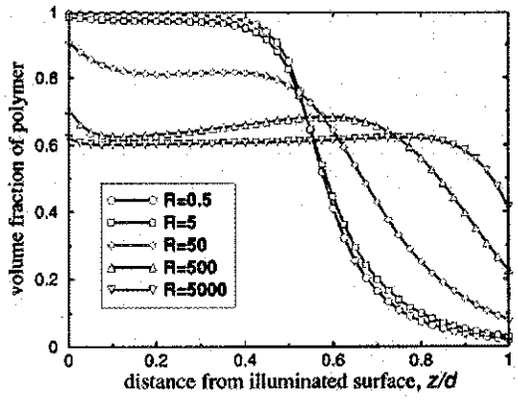

Fig. 3. Final volume fraction of polymer, which shows better separation for slower polymerization.

When the UV is irradiated, it is predominantly absorbed by the LCs, so a gradient intensity in z-axis is generated in the mixture. As a consequence, the polymerization rate is higher close to the illuminated region and thus more prepolymers are cross-linked in here. Thus, a gradient of the prepolymer concentration is produced, and this leads to a migration of the prepolymers from the bulk to the illuminated area. It caused the chain reaction of LC's migration in the opposite direction. The migration of small molecules (prepolymer and LC) is much faster than that of the large polymers, which eventually form the immobile polymer structure. The LCs moves with diffusion from the concentration change and the prepolymers undergo diffusion, then consumed by the polymerization. In this analysis, the polymer is treated as immobile, but has a local volume fraction that keeps growing before the end of the polymerization. Fig. 3 shows the numerical calculation with various relative polymerization rate, defined as R which is proportional to the UV intensity at z=0 [8]. The result shows that slow polymerization, represented by small values of R, leads to a more sharply defined boundary. The importance of slow polymerization to phase separation is thus clearly illustrated and these experimental observations are at least in qualitative agreement with the numerical results.

One interesting point is that the presence of an alignment layer on the substrate in contact with the LC will enhance the formation of uniform layers. Recently, we had reported that the morphology after phase separation is greatly affected by the surface interaction between the LC/pre-polymer and surface layer [10]. By optical microscopic studying of phase separation for various monomers, it was found that the resultant structures depend not only on bulk properties of the LC/monomer but also on the surface interaction with the surface layer. According to this model, a PSCOF structure is obtainable at even higher UV intensity (i.e., faster phase separation) with proper alignment layers which has higher wettability with LC than prepolymer. This suggests that the LCs near the alignment layer respond to its anchoring potential and align parallel to the rubbing direction. The volume of aligned LC grows during the phase separation

process. Oriented LC molecules determine the microscopic structure of the polymer-LC interface which becomes compatible with their alignment.

In summary, through the control of the UV illumination and the use of a photomask, various structures of the polymer such as micro-walls or micro-relief arrays can be produced with the LC/prepolymer composites. The resultant polymer structures can be used for constructing various LC-based EO devices such as flexible displays and active microlenses. In the presence of the polymer structures formed by the photo-reaction, the mechanical stability of such devices will be much improved.

3. PHASE SEPARATION FOR FLEXIBLE DISPLAYS

3.1 Device Configuration and Fabrication

In recent years, LC devices using plastic film substrates have drawn much attention for use in portable applications such as smart cards, cellular phone, and PDA because of their lighter weight, thinner packaging capability, flexibility, and lower manufacturing cost through continuous roll-to-roll process. Different EO modes have been proposed for plastic liquid crystal displays (LCDs) [11]. However, since plastic substrates do not give solid mechanical supports for the LC alignment, polymer walls and/or networks as supporting structures have been proposed and demonstrated [1,12]. These structures were fabricated using an anisotropic phase separation method from the polymer and the LC by applying a patterned electric field or spatially modulated UV light. However, a high electric field is needed to initiate the anisotropic phase separation or residual polymers, decreasing the quality of displays, remain in an unexposed region.

We proposed the pixel-isolated LC (PILC) structure to guarantee a stable LC structure under external distortion through the anisotropic phase separation [2,3]. In this structure, the LC molecules are isolated in pixels surrounded by inter-pixel vertical polymer walls and horizontal polymer films on the substrate. As a result, a good mechanical stability is obtained without diminishing the EO properties of the LC device.

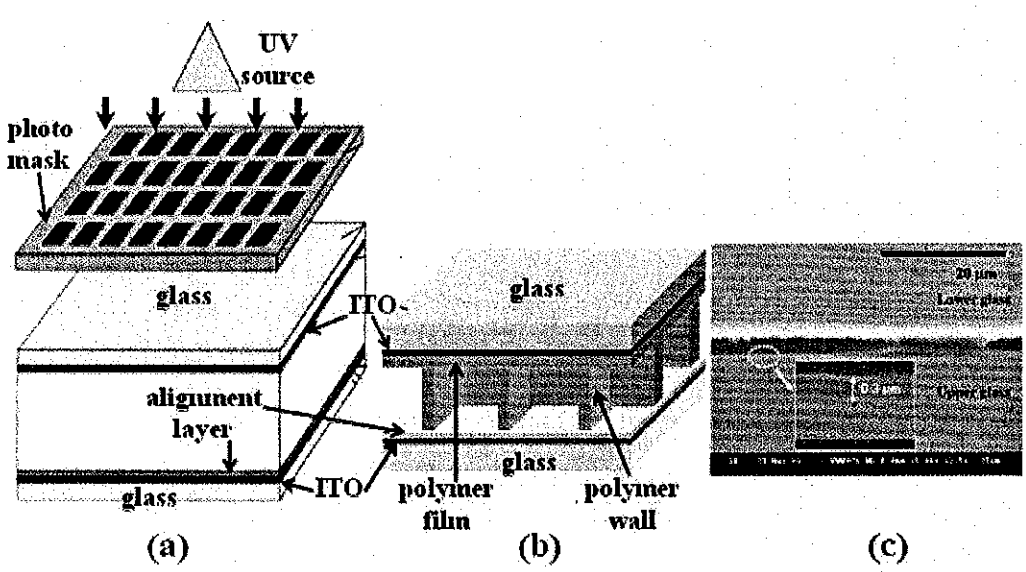

Fig. 4. Schematic diagram of (a) fabricating PILC structure by anisotropic phase separation, (b) the resultant device configuration upon the UV exposure and (c) cross-sectional SEM image.

Figure 4 shows the fabrication process of a PILC structure. The cell with the LC/monomer mixture was irradiated by the UV light through a photomask with two-dimensional rectangular patterns that block the UV transmission as depicted in the Fig. 4(a). With the UV irradiation, the polymer walls were formed in the high intensity region. As shown in Fig. 4(b), the polymer walls were produced along the z-direction (vertical) on the substrate. After removing the photomask, the subsequent UV exposure was performed to fully harden the polymer. During this process, the second phase separation of the LC molecules and the polymers was accompanied and the polymer layer was formed in the x-y plane on the illuminated substrate (i.e. the upper substrate in Fig. 4(a)). Figure 4(b) shows the resultant structure through two anisotropic phase separation processes by the two-step UV exposure. The magnified image in the Fig. 4(c) shows the vertical polymer walls in inter-pixels and horizontal uniform polymer films on the upper substrate. These polymer structures separate the LC from neighboring pixels and act as patterned spacers. In principle, the PILC mode can be applicable for various LC phases such as the nematic, the ferroelectric, and the cholesteric phases. Note that the phase-separated LC textures depend on the wetting properties of both the monomer and the LC on the alignment layer.

3.2 Experimental

Two indium tin oxide (ITO)-coated poly(ether sulfone) films of 200 μm thick were used as flexible substrates. It was found that the PILC structures were well formed on these plastic substrates. Figure 5 shows the textural changes of a standard LC cell (with no polymer structures) and a PILC cell on plastic substrates in the presence of external point pressure generated with a sharp tip. The LC alignment in the standard cell was severely deformed due to the variation of the cell gap as shown in Fig. 5(a). Such deformation propagates over a quite large area and results in the degradation of the EO properties. In contrast, the PILC cell exhibits no appreciable change since the LC molecular reorientation is restricted in pixels by the vertical polymer walls and the horizontal polymer layer as shown in Fig. 5(b). The dispersed small dots were glass spacers.

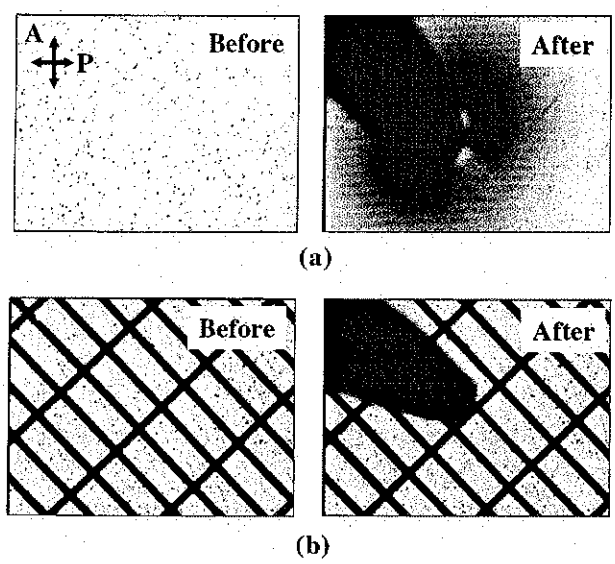

Fig. 5. Microscopic textures of a standard LC cell and a PILC cell with plastic substrates: (a) before and after point pressure on a standard LC cell and (b) before and after point pressure on a PILC cell.

3.3 Mechanical Stability under Bending Condition

Now we examine the mechanical stability of the PILC cell under bending states. The cell was bent using a pair of linear translation stages and placed between two crossed polarizers. The degree of bending is typically represented by the curvature of the cell (R) which can be defined in the experimental set-ups shown in the Fig. 6(a) and (b). As R decreases, the degree of bending is increased. The measured transmittance for the PILC cells is shown as a function of the applied

voltage for various bending states in Fig. 6(c). Under bending deformation, the PILC cell shows nearly the same behavior in a wide range of the applied voltage except for the low voltage regime as shown in Fig 6(c). It is clear that LC molecular distortions due to the bending stress are effectively reduced in the PILC LC cell. Moreover, the PILC cell has no appreciable shift of the threshold voltage, which is different from a polymer-network or a polymer-dispersed LC cell where the threshold voltage increases with the polymer concentration. [13].

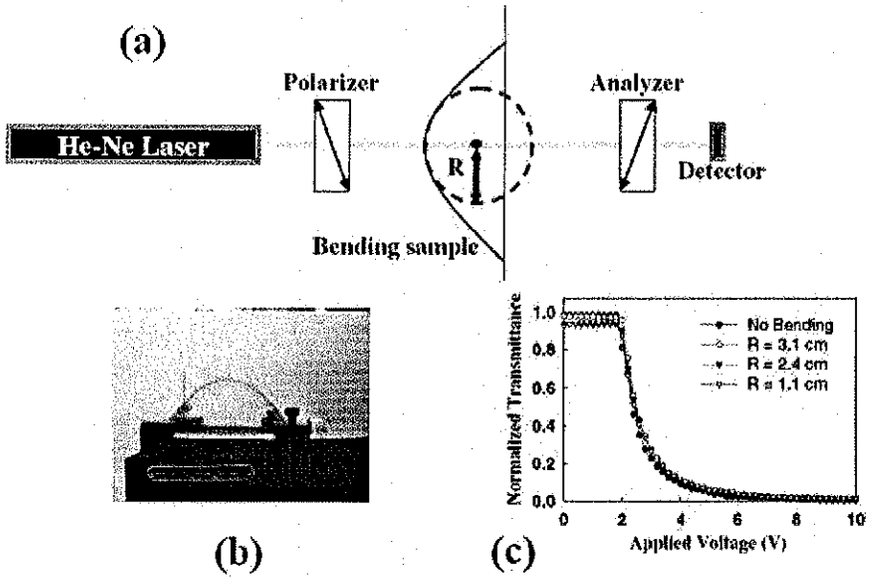

Fig. 6. (a) Experimental setup for bending test (b) Photograph of experiment (c) Normalized transmittance vs the applied voltage for the PILC cell in various bending states. The radius of curvature R represents the degree of bending.

Figure 7 shows a prototype PILC cell of the size of 3 inch under the bending state. In bent circumstances, the alignments of LCs are stable as we observed in the magnified photograph in the inset. These PILC structures formed by a photo-induced anisotropic phase separation would play an important role in fabricating high-performance flexible LC displays.

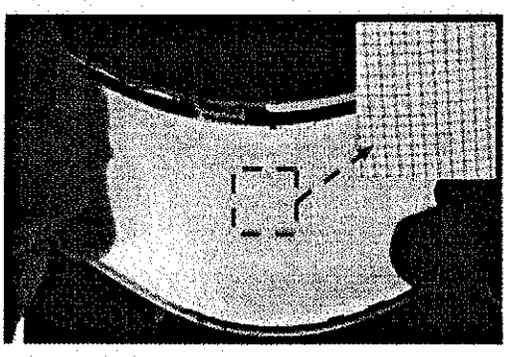

Fig. 7. A prototype PILC cell of 3 inch, fabricated on the PILC structures.

4. ACTIVE MICROLENS ARRAYS USING PSCOF STRUCTURE

4.1 Fabrication and Operational Principle

With the advancement in optical computing and communications technology, there is a growing need for real-time reconfigurable optical elements such as fast optical switches, beam-steering (e.g., diffractive gratings), and wave-front-shaping (e.g., microlens arrays) devices in high-density data storage, optical interconnects, and beam-modulating and energy-directing applications [5,14,15]. In this section, we introduce the fabrication of microlens array with a nematic LC (NLC) and a ferroelectric LC (FLC) by using the anisotropic phase separation method [4-6]. The NLC-based device has an electrically variable focal length in milliseconds while the FLC-based microlens array exhibits the memory effect and modulates the transmitted light within a few microseconds.

Table. 1. Summary of the ordinary and extraordinary refractive indices of the used materials at 590 nm.

Materials	Ordinary (n_o)	Extraordinary(n_e)
E-31	1.533	1.792
Felix 15-100	1.490	1.664
NOA 65	n_p=1.524	

The materials used in this study are commercial nematic E-31 (Merck Chemical Company, Germany), ferroelectric Felix 15–100 (Clariant, Germany), and photocurable prepolymer NOA-65 (Norlandproduct, USA). In Table I, we summarize the ordinary and extraordinary refractive indices for the materials we used. Cell gap is maintained with the glass fiber or bead spacers of 5–25-μm (NLC case), 3 μm (FLC case) diameter. To align the LC, we spin-coat and then rubbed the thin films of poly–vinyl–alcohol (NLC case) or Nylon 6 (Sigma Aldrich, USA) (FLC case). We note that the results of phase separation are greatly affected by the alignment layer and the type of prepolymer. A solution of the LC and prepolymer, in the weight ratio of 60:40, is injected into the cell by capillary action at the temperature which exhibits the isotropic phase of the LCs. The cells are exposed to UV light of 350 nm to initiate polymerization. The source of the UV light is a Xenon lamp operated at 200 W.

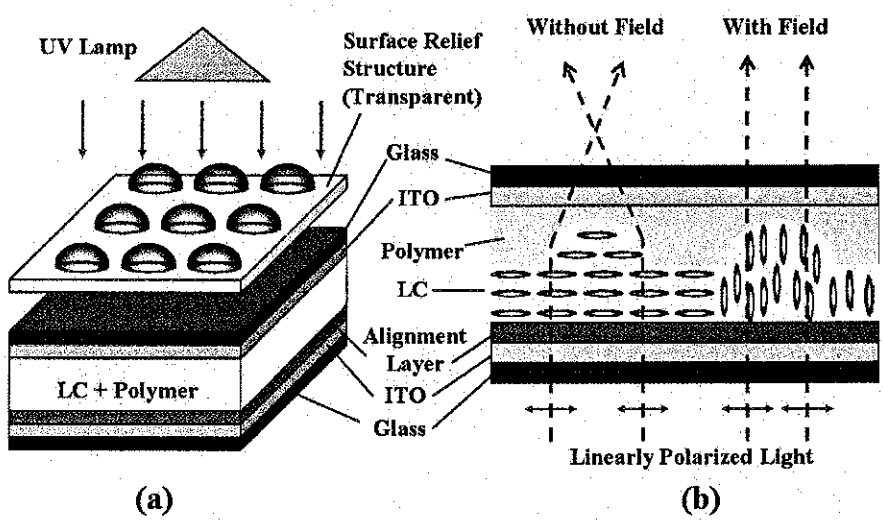

Fig. 8. (a)Fabrication of LC microlens array using phase separation effect with the pre-designed surface relief structure (b) Schematic diagram of a device configuration of NLC microlens and their two operating states.

The LC microlens we proposed can be simply obtained by modulating an irradiated UV light. Figure 8(a) shows the fabrication process schematically. We use a surface relief structure of hemispheres as a transparent photomask. The surface relief structure is placed on the top glass substrate. Then, the cell with the mixture of a LC and a prepolymer is irradiated with UV light for ~ 10 minutes. A second exposure is performed without the relief structure for 5 minutes to fully harden the polymer. During this process, the LC molecules that remain in the polymer network after the first UV exposure are expelled from the polymerized volume. Because of the thickness-dependent absorption, a UV intensity gradient is created across the circular areas during the anisotropic phase separation which results in the highest LC concentration in the middle of the shadow. After the complete polymerization, a three-dimensional plano-convex structure of the polymer is created on the top glass substrate as shown in Fig. 8(b). The homogeneous planar alignment of LCs is obtained by a unidirectional rubbing of the bottom alignment layer. Both NLC and FLC cases have the same device structure except for the direction of the molecules during driving. Here, we first described the characteristics of the NLC device.

The resultant NLC-based microlens configuration is schematically shown in Fig. 8(b) [6]. For the incident light with the polarization parallel to the director of the NLC, the beam will be focused due to the refraction at the curved boundary in the absence of an applied voltage. Under an applied voltage, the director of the NLC reorients perpendicular to the substrate and the incident beam simply passes through the LC cell without refraction if the refractive indexes of two mediums, the NLC and the polymer, are identical.

In the simple optical model [16], the focal length f of the NLC microlens can be given in terms of the radius of curvature (R) of the curved morphology, the effective refractive index of the LC (n_{lc}), and that of the polymer (n_p) as follows [4].

$$f = \frac{R}{n_{lc}(V) - n_p}.$$

The effective refractive index of the NLC is written as [17].

$$n_{lc}(V) = \frac{n_e n_o}{\sqrt{n_e \sin^2 \theta(V) + n_o \cos^2 \theta(V)}},$$

where $\theta(V)$ is the polar tilt angle of the LC as a function of the applied voltage. This means that the focal length of a NLC-based microlens can be electrically tuned.

4.2 Characteristics of NLC Microlens

Figure 9 shows the focusing properties of the NLC microlens for an incident beam a He-Ne laer with the wavelength of 632.8 nm. The polarization of the incident beam is parallel to the LC director. Figure 9(a) is the image of the beam focused by a microlens under no applied voltage. The NLC microlens acts as a convex lens with the focal length of 1.7 mm. The light intensity profile measured at the focal point is presented in Fig. 9(b). At the applied voltage of 3 V, the beam was defocused at a distance of 1.7 mm as shown in Fig. 9(c) while refocused at 3.7 mm as shown in Fig. 9(d).

In next, we examined the tuning characteristics of the focal length. The variation of the focal length with the applied voltage is shown in Fig. 10. The focal length was found to depend quadratically on the voltage above the threshold of 1.5 V. The field-on and field-off switching times were found to be 30 ms and 130ms, respectively. From the measured curvature $R = 381 \pm 20$ μm, the focal length was calculated as 1.6±0.1 mm, which is in good agreement with the measured value of 1.7 mm. The diameter of single LC microlens was about 100μm.

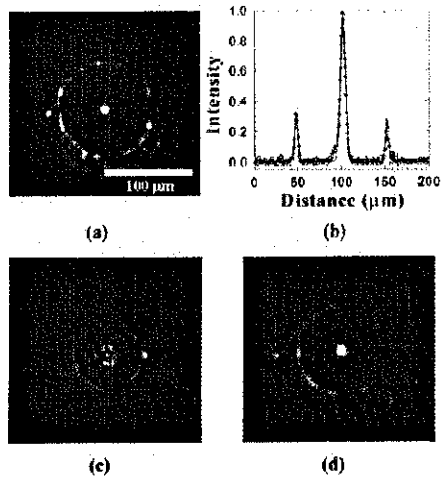

Fig. 9. Focusing properties of the NLC microlens for an incident laser beam: (a) focused beam image at 1.7 mm under no applied voltage, (b) light intensity profile at the focal point, (c) defocused beam image at 1.7 mm under 3 V, and (d) refocused beam image at 3.7 mm under 3 V.

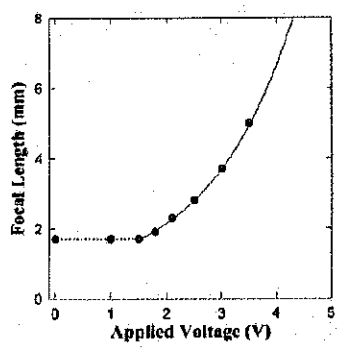

Fig. 10. Voltage dependence of the microlens' focal length. Focal length increases quadratically for fields higher than the threshold value of 1.5 V.

4.3 FLC Microlens Device

For fast switching LC-based microlens, FLC materials have been widely used [6, 37]. In FLCs, the spontaneous polarization is directly coupled with an external electric field and results in fast response. In a surface-stabilized FLC geometry [18], two stable states exist and the memory effect is produced. The bistable switching between the two states is driven by the polarity of an applied electric field. The FLC used in this study is known to have a good alignment for the surface-stabilized FLC mode with a rather long pitch (28 μm).

Figure 11 shows the focusing properties of a FLC microlens array for an incident laser beam. The diameter of each microlens is 335 μm. At the applied of voltage 10 V, the focal length was found to be 11 mm, and the focused beam was shown in the Fig. 11(a). When the polarity of the electric field was reversed, the focused image became blurred as shown in the Fig. 11(b). When the electric field was off from ±10 V, the image in the Fig. 11(a) and that in the Fig. 11(b) appeared as shown in the Fig. 11(c) and the Fig. 11(d), respectively. The intensity profiles of the four images are shown in the Fig. 11(e). It is clear that the FLC microlens possesses the memory effect with a light change in the light intensity. The slight change is believed due to the remaining polymer in the FLCs. The switching times for the on-state and the off-state were measured as 150 μm and 88 μs, respectively. These times are about 1000 times faster than the NLC case.

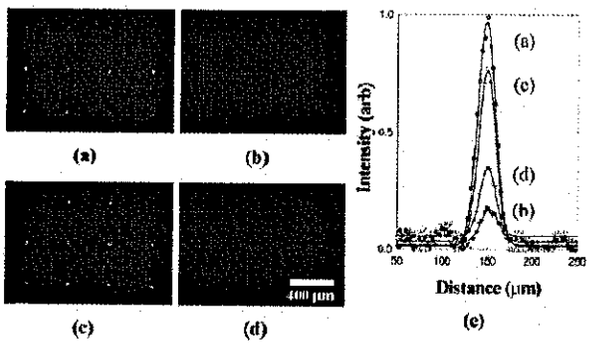

Fig. 11. Focusing characteristics of the FLC microlens for an incident laser beam: (a) the beam image under 10 V at 11 mm, (b) that under -10 V at 11 mm, (c) the beam image under 0 V switched from + 10 V, (d) that under 0 V switched from - 10 V, and (e) the intensity profiles for (a) to (d).

5. CONCLUSION

We have introduced the physical understanding of the anisotropic phase separation of LC/polymer composite based on the one-dimensional kinetic approach. As the application of PSCOF structure, the flexible displays with PILC structure and the microlens array with tuning capability were demonstrated. The phase-separated LCs with polymer structures such as polymer walls and microlens, formed through the photo-induced anisotropic phase separation, would be very useful for developing photonic devices and flexible displays.

ACKNOLEDGEMENT

This work was supported in part by Samsung Electronics co. Ltd. and the Korea Research Foundation Grant funded by the Korean Government (MOEHRD) (KRF-2007- 005-J04104).

REFERENCES

1. V. Vorflusev and S. Kumar, "Phase-separated composite films for liquid crystal displays," Science **283(5409)**, 1903-1905 (1999).
2. J.-W. Jung, S.-K. Park, S.-B. Kwon and J.-H. Kim, "Pixel-isolated liquid crystal mode for flexible display applications," Jpn. J. Appl. Phys. **43(7A)**, 4269-4272 (2004).
3. J.-W. Jung, M. Y. Jin, H.-R. Kim, Y.-J. Lee and J.-H. Kim, "Mechanical stability of pixel-isolated liquid crystal mode with plastic substrates," Jpn. J. Appl. Phys. **44(12)**, 8547-8551 (2005).
4. H.-S. Ji, J.-H. Kim and S. Kumar, "Electrically controllable microlens array fabricated by anisotropic phase separation from liquid-crystal and polymer composite materials," Opt. Lett. **28(13)**, 1147-1149 (2003).
5. J.-H. Kim and S. Kumar, "Fast switchable and bistable microlens array using ferroelectric liquid crystals," Jpn. J. Appl. Phys. **43(10)**, 7050-7053 (2004).
6. J.-H. Kim and S. Kumar, "Fabrication of electrically controllable microlens array using liquid crystals," J. of Lightw. Technol. **23(2)**, 628-632 (2005).
7. P. S. Drzaic, Ed., *Liquid Crystal Dispersions*, World Scientific, Singapore, 1995.
8. T. Qian, J.-H. Kim, S. Kumar and P. L. Taylor, "Phase-separated composite films: Experiment and theory," Phys. Rev. E. **61(4)**, 4007-4010 (2000).

9. V. V. Krongauz, E. R. Schmelzer and R. M. Yohannan, "Kinetics of anisotropic photopolymerization in polymer matrix," Polymer **32**, 1654 (1991).
10. M. Y. Jin, T.-H. Lee, J.-W. Jung and J.-H. Kim, "Surface effects on photopolymerization induced anisotropic phase separation in liquid crystal and polymer composites," Appl. Phys. Lett. **90(19)**, 193510 (2007).
11. G. P. Crawford, Ed., *Flexible Flat Panel Displays*, John Wiley & Sons, Chichester, 2005.
12. Y. Kim, J. Francl, B. Taheri and J. L. West, "A method for the formation of polymer walls in liquid crystal/polymer mixtures," Appl. Phys. Lett. **72(18)**, 2253-2255 (1998).
13. P. A. Kossyrev, J. Qi, N. V. Priezjev, R. A. Pelcovits and G. P. Crawford, "Virtual surfaces, director domains, and the Fréedericksz transition in polymer-stabilized nematic liquid crystals," Appl. Phys. Lett. **81(16)**, 2986-2988 (2002).
14. Y. Choi, J.-H. Park, J.-H. Kim and S.-D. Lee, "Fabrication of a focal length variable microlens array based on a nematic liquid crystal," Opt. Mater. **21**, 643-646 (2002).
15. Y. Choi, C.-J. Yu, J.-H. Kim and S.-D. Lee, "Fast switching characteristics of surface-relief microlens array based on a ferroelectric liquid crystal," Ferroelectrics **312**, 25-30 (2004).
16. B. E. A. Saleh and M. C. Teich, *Fundamentals of Photonics*, John Wiley & Sons, New York, 1991.
17. P. Yeh and C. Gu, *Optics of Liquid Crystal Displays*, John Wiley & Sons, New York, 1999.
18. N. A. Clark and S. T. Lagerwall, "Submicrosecond bistable electro-optic switching in liquid crystals," Appl. Phys. Lett. **36(11)**, 899-901 (1980).